

Alma Mater Studiorum Università di Bologna
Archivio istituzionale della ricerca

Lichens as monitors of the atmospheric deposition of potentially toxic elements in high elevation Mediterranean ecosystems

This is the final peer-reviewed author's accepted manuscript (postprint) of the following publication:

Published Version:

Vannini A., Tedesco R., Loppi S., Di Cecco V., Di Martino L., Nascimbene J., et al. (2021). Lichens as monitors of the atmospheric deposition of potentially toxic elements in high elevation Mediterranean ecosystems. SCIENCE OF THE TOTAL ENVIRONMENT, 798, 1-8 [10.1016/j.scitotenv.2021.149369].

Availability:

This version is available at: <https://hdl.handle.net/11585/856203> since: 2022-02-11

Published:

DOI: <http://doi.org/10.1016/j.scitotenv.2021.149369>

Terms of use:

Some rights reserved. The terms and conditions for the reuse of this version of the manuscript are specified in the publishing policy. For all terms of use and more information see the publisher's website.

This item was downloaded from IRIS Università di Bologna (<https://cris.unibo.it/>).
When citing, please refer to the published version.

(Article begins on next page)

This is the final peer-reviewed accepted manuscript of:

Andrea Vannini, Raffaello Tedesco, Stefano Loppi, Valter Di Cecco, Luciano Di Martino, Juri Nascimbene, Federico Dallo, Carlo Barbante, Lichens as monitors of the atmospheric deposition of potentially toxic elements in high elevation Mediterranean ecosystems, Science of The Total Environment, Volume 798, 2021, 149369

The final published version is available online at:
<https://doi.org/10.1016/j.scitotenv.2021.149369>

Terms of use:

Some rights reserved. The terms and conditions for the reuse of this version of the manuscript are specified in the publishing policy. For all terms of use and more information see the publisher's website.

This item was downloaded from IRIS Università di Bologna (<https://cris.unibo.it/>)

When citing, please refer to the published version.

Morphotectonics and late Quaternary seismic stratigraphy of Lake Garda (Northern Italy)

Luca Gasperini^{a,*}, Alfredo Marzocchi^b, Stefano Mazza^b, Roberto Miele^a, Matteo Meli^a, Hassan Najjar^a, Alessandro M. Michetti^c, Alina Polonia^a

^a Istituto di Scienze Marine (ISMAR), CNR, Marine Geology, Bologna, Italy

^b Università Cattolica del Sacro Cuore, Brescia, Italy

^c Università degli Studi dell'Insubria, Como, Italy

ARTICLE INFO

Article history:

Received 17 June 2020

Received in revised form 8 September 2020

Accepted 8 September 2020

Available online xxx

Keywords

Lake Garda

Quaternary seismic stratigraphy

Alpine chain

Seismic facies

Earthquake hazards

Megaturbide-Homogenite beds

ABSTRACT

Lake Garda, the largest lake in Italy at the southern front of the central Alps, provides a unique opportunity to reconstruct Quaternary geological processes related to the interplay between deglaciation driven sedimentation and tectonic activity. In fact, the topographic depression presently occupied by the lake was site of a major glacial tongue during the LGM, and is located close to the epicentral areas of two of the largest magnitude historical earthquakes recorded in the Po Plain, the Verona (Jan. 13, 1117) and Brescia, (Dec. 25, 1222) seismic events, characterized by Io IX-X MCS, respectively. Despite this peculiarity, geophysical surveys of the lake are scant. We present results of a waterborne geophysical survey of Lake Garda, leading to the acquisition of a densely-spaced grid of high-resolution seismic reflection profiles which image the lake floor and uppermost sedimentary sequence. These data enabled us to compile thematic maps which provide insights on active geologic processes in different sectors of the basin. We focused our work on a prominent seismic reflector (H1), correlated over the entire lake surface, to estimate the sediment deposition rate at the scale of the last 10 ka, and to evaluate the variability of seismic facies and geological processes in different sectors of the basin. Based on available stratigraphic data, we discuss whether H1 could mark the diachronic glacial/fluvio-glacial transition after the Last Glacial Maximum, when the ice tongues south of the Alps started to melt and collapse. We observed that sediments of the southern Lake Garda are affected by incipient tectonic deformation, and two major seismoturbidite-homogenite beds might represent over 50% of the Holocene sedimentary record in the lake depocenter, making the study of the Lake Garda stratigraphy an interesting tool for assessing earthquake hazards at the southern front of the Alpine chain.

© 2020

1. Introduction

Lake Garda, in northern Italy (Fig. 1), is a valuable natural heritage and an important touristic target, as well as the primary reservoir of fresh water in the Italian Peninsula. Known since ancient times with the name of *Benaco*, the lake is located at the foot of the Alpine chain, in a tectonic depression shaped by exogenous processes. It is the largest lake in Italy (about 370 square kms of surface), is located 65 m above the mean sea level, and reaches a maximum depth of over 345 m.

Morpho-bathymetric and reflectivity data obtained with modern geophysical techniques, such as chirp sonars, calibrated echo sounders, and algorithms to infer geological properties of the sediments based on their acoustic response (reflectivity, sound velocity, coherence, etc.),

are essential tools for studying natural and anthropogenic processes involved in the evolution of lacustrine basins. These data could help in detecting the effect of geological variables at different space and time scales, either episodic, such as slumps and landslides, or steady-state, as the continuous deposition of sediments delivered to the basin by river inflows and eventually reworked by bottom currents. Information on natural and anthropic processes affecting the lake stratigraphy generally leads to important insights regarding the evolution of the basin itself and of its surroundings. Lacustrine records represent important historical/prehistorical archives that could help in protecting, managing and sustainably exploiting these important resources (Saulnier-Talbot, 2016, and references therein). Despite its importance, Lake Garda has been poorly studied using such techniques, and geophysical imaging of its floor and sedimentary infill are scant (e.g., Curzi et al., 1992; Berlusconi et al., 2013). This prevents the possibility of reconstructing the lake's evolution and deciphering the effects of active sedimentary and tectonic processes which continuously reshape its floor, as

* Corresponding author.

E-mail address: luca.gasperini@ismar.cnr.it (L. Gasperini)

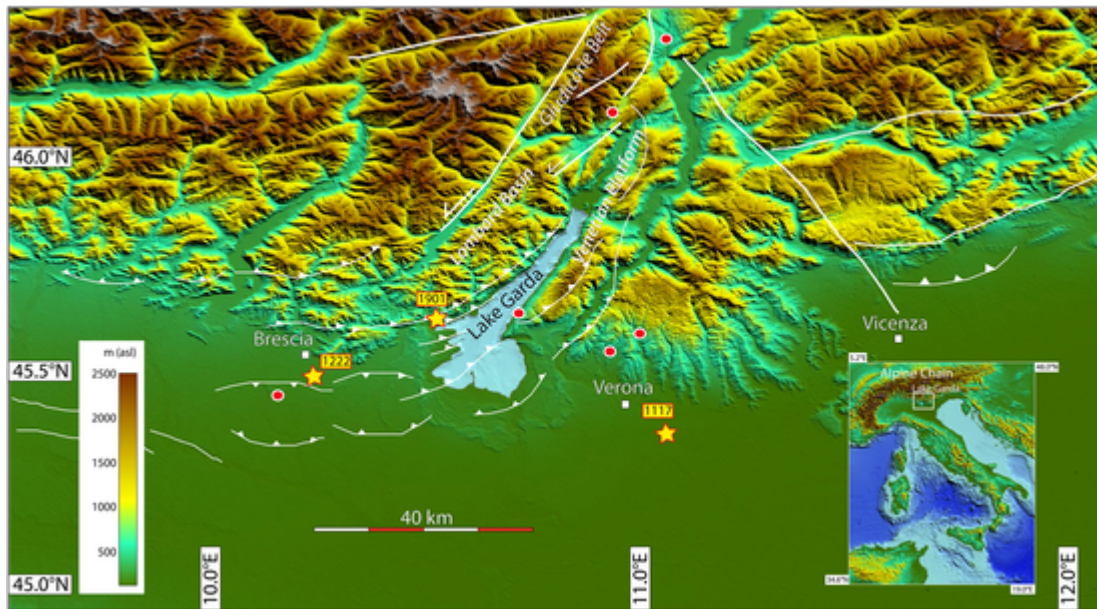


Fig. 1. Quaternary active thrust belt of the Central Po Plain and adjacent South Alpine Domain (modified after Berlusconi et al., 2013). Yellow stars mark the epicenters of strong historical earthquakes, including the January 3, 1117, December 25, 1222, and October 30, 1901, events (epicentral locations modified from Magri and Molin, 1986; Guidoboni and Comastri, 2005; Galli, 2005; Guidoboni et al., 2005, 2019; Stucchi et al., 2008; Livio et al., 2009). Red circles indicate sites showing evidence of historical or paleoseismic earthquake surface ruptures (from Sauro, 1992; Galadini and Galli, 1999; Sauro and Zampieri, 2001; Galadini et al., 2001; Livio et al., 2019). Morphology is from ASTER Global Digital Elevation model (doi: <https://doi.org/10.5067/ASTER/ASTGTM.003>). (For interpretation of the references to colour in this figure legend, the reader is referred to the web version of this article.)

amount and quality of sediment supplied by rivers, sediment reworking caused by differences in temperature between the lake's and the river's waters, frequency and distribution of subaqueous mass wasting and landslide events triggered by river floods, earthquake shaking and other gravitative processes.

In this paper, we present results of a waterborne geophysical survey of Lake Garda that acquired a densely-spaced grid of high-resolution seismic reflection profiles which of the lake floor and uppermost sedimentary sequence, which highlights a complex interplay between geological processes at different scales during the late Pleistocene-Holocene.

2. Geographic and geologic setting

Lake Garda extends along a NNE/SSW oriented axis, with a maximum length of 52 km, and widths ranging from about 3 km in the northern sector, to 16 km in the south wider basin. The main inflow is represented by River Sarca, at the northern end of the lake. Other tributaries are of less importance and mainly located along the western and northern coasts (Fig. 2). The emissary is River Mincio, with a discharge of about $58 \text{ m}^3/\text{s}$, a low value if compared with those reported for the other two largest Insubrian lakes (Maggiore, $296 \text{ m}^3/\text{s}$ and Como, $158 \text{ m}^3/\text{s}$), and is due to Lake Garda's small drainage basin (Salmaso and Decet, 1998), formed after a late-glacial diversion of the River Adige (Cremaschi, 1994). Annual rainfall in the catchment area is in the order of 1200 mm. The Lake Garda relatively long water renewal time, about 27 years for the entire basin, is distinctive among the deep southern subalpine lakes, and the combination of largest area and smaller drainage basin would suggest an Holocene sedimentation rates lower than the other subalpine lakes, such as Lake Como and Lake Maggiore (Curzi et al., 1992; Lehmann et al., 2002; Calderoni, 2003; Fanetti et al., 2008). The NE-SW oriented and rectilinear northern lake shores are characterized by high topographic gradients and rocky cliffs, while the southern broader sector shows gentler morphologies due to the presence of moraine hills (Fig. 2).

Lake Garda is located in the central part of the Southern Alps (Fig. 1), a vast tectonic unit mainly characterized by the Dolomia Principale

formation and generally E-W trending folds (Castellarin et al., 1992). Structural elements were formed or reactivated in this area, during the last phase of the Alpine orogenesis, which occurred between 29–25 Ma and 10–7 Ma. (Doglioni and Bosellini, 1987; Picotti et al., 1995; Fuganti et al., 2001; Castellarin et al., 2006).

The lake depression is located between two major tectonic units, the Lombard Basin to the west, and the Venetian Platform to the east (Fig. 1). A NNE-SSW tectonic feature named the Ballino-Garda line, delimits the two. This represents a Mesozoic scarp of vertical normal faults, which accommodated the lowering of the western section during Jurassic-Cretaceous period, leading to the formation of a shallow sea on the Venetian Platform, which gradually deepened towards the Lombard Basin, determining the deposition of limestones, dolostones and chalk from east to west (Castellarin and Ferrari, 1972; Castellarin, 1982; Fuganti et al., 2001; Trombetta et al., 2004). Around the lake shores, the dolostones of the Dolomia Principale represent predominant lithologies (Trombetta et al., 2004). According to available catalogues (Camassi et al., 2011; Guidoboni et al., 2019; Rovida et al., 2020), the Lake Garda surroundings were struck by intense seismicity during historical times, including the Jan. 13, 1117, Verona (Io = IX-X MCS; Mw 6.9); the Christmas 1222, Brescia (Io = VII-IX MCS; Mw 6.0); and the Oct. 30, 1901 Salò (Io = VIII MCS, Mw 5.7) earthquakes (Fig. 1). Indeed, Lake Garda falls in the epicentral area of the largest seismic events recorded in the Po Plain, generated along reverse faults (Serva, 1990; Galadini and Galli, 1999; Livio et al., 2009; Berlusconi et al., 2013; Viganò et al., 2015). In the Po Plain foredeep, the recurrence interval of strong earthquakes is long, probably in the order of one to several thousand years, while typical slip-rates for Quaternary faults is $<1 \text{ mm/year}$, much lower than typical erosion rates in the glaciated piedmont belt (Michetti et al., 2012; Berlusconi et al., 2013; Livio et al., 2014). For this reason, reconstructing the interplay between tectonics and sedimentation would require high resolution data, such as those characterizing the Lake Garda sedimentary sequence, which for this reason could represent an important archive for historical and pre-historical seismicity.

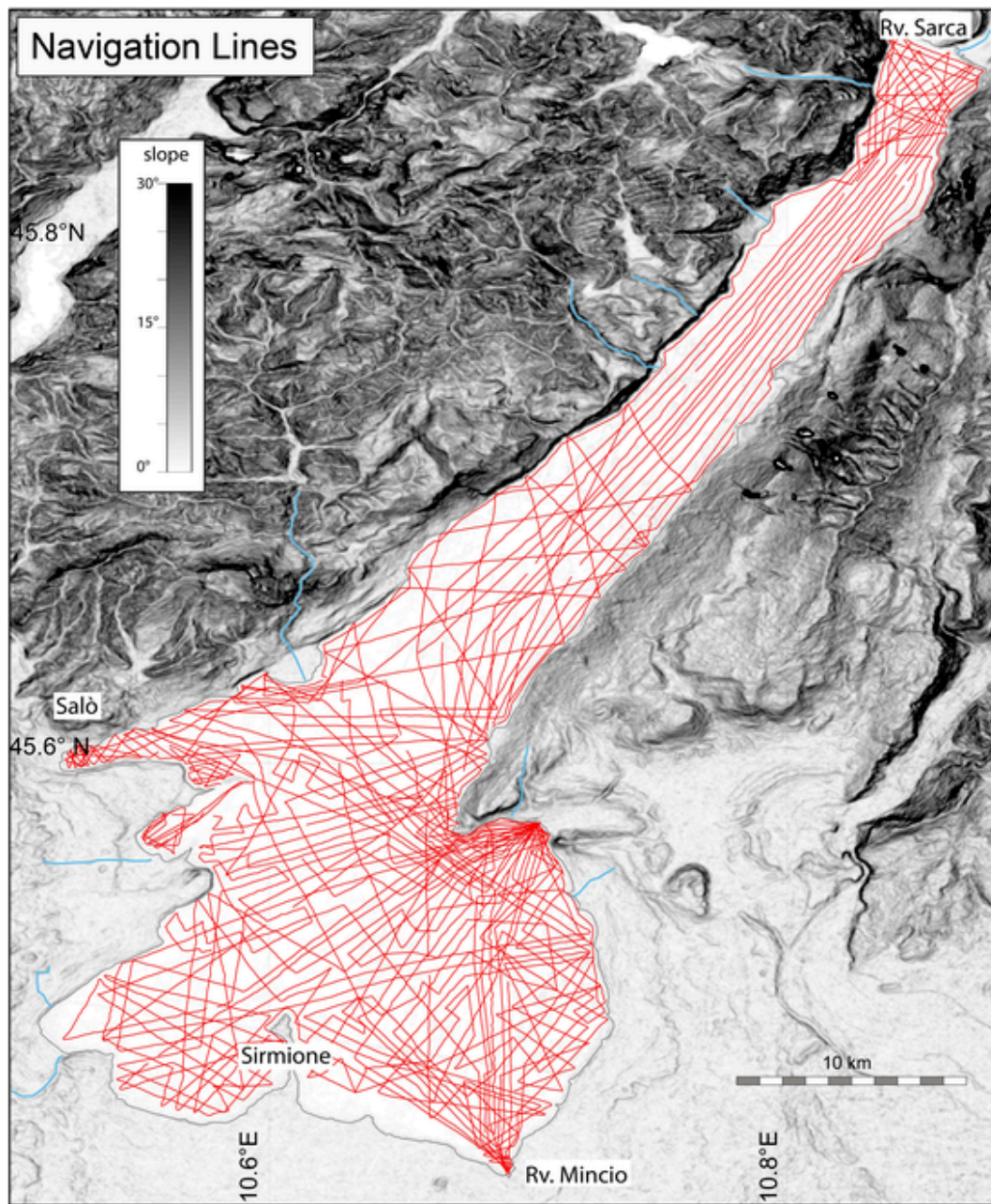


Fig. 2. Slope map of the Lake Garda surroundings compiled using the ASTER global grid digital elevation dataset (<https://asterweb.jpl.nasa.gov/gdem.asp>). Coverage of high-resolution seismic reflection profiles collected during the 2017 survey is marked by red lines. Main inflowing rivers are indicated by pale-blue lines. (For interpretation of the references to colour in this figure legend, the reader is referred to the web version of this article.)

Lake Garda, as other major Alpine lakes, occupies a glacially over-deepened basin (Bini et al., 1978; Preusser et al., 2010) dammed by composite end-moraine systems, mostly built up during the Last Glacial Maximum, from 30 to 18 ka cal BP (Schaefer et al., 2006). Continuous stratigraphic lake records preserved in several sedimentary archives, reveal the ecological history of de-glaciated terrains, and provide proxies for climate events triggering the last glacial/interglacial transition (Schmidt et al., 2012; Ammann et al., 2013; Ravazzi et al., 2014; Monegato et al., 2017). The post LGM evolution and collapse of the Garda glacier have been reconstructed using cores collected from lacustrine sediments onshore, while the only available seismo-stratigraphic data on the Holocene lacustrine deposits previous to our survey were relatively sparse high-resolution seismic reflection and refraction data collected in 1992 (Curzi et al., 1992). While

previous

reconstructions were mainly focused on finding offshore extensions of active faults detected onshore, taking advantage by our densely-spaced grid we tried to image the geometrical complexity of tectonic deformations recorded in the sedimentary sequence.

3. Methods

Data presented in this paper were collected during a campaign carried out by ISMAR-CNR (Bologna) in, cooperation with Università Cattolica del Sacro Cuore (Brescia, Italy) in November/December 2017. For this survey, we employed a motorboat equipped with a single beam echo sounder and Benthos-Teledyne CHIRP III chirp subbottom profiler, which allowed the acquisition of a close-spaced grid of high-resolution seismic reflection profiles (Fig. 2). Acquisition along the water column of the main physical parameters, including temperature, pres-

sure and conductivity, was carried out at the lake center at the beginning and end of the survey, in order to obtain average sound propagation speed values to convert TWT (two-way travel times) into depth. After data processing, calibration, and analysis, which included editing of the soundings, semi-automatic picking of the sediment-water interface, and depth conversion by means of sound velocity profiles, we compiled a morphobathymetric and a reflectivity map of the lake floor. We then focused on a seismic reflector (H1) which was correlated through the different sectors of the lake, seemingly marking a dramatic change in the depositional environment.

3.1. Data acquisition

The highly-repeatable frequency-modulated signal generated by the seismic source, as well as the choice of constant emission power and receiver gain during the entire survey, led us to estimate the lake-floor reflectivity, and use such parameters as diagnostic of sediment distribution. The chirp sonar system was equipped with two electro-acoustic transducers connected in parallel, both employed as transmitters and receivers. The pulse length was set to 15 msec., while the transmission frequency was a sweep between 2 and 7 kHz. The motorboat speed during the survey was around 5 knots, while the shooting rate varied between 125 and 750 ms., depending by water depth. The received signal was deconvolved and processed in real time by the acquisition system and stored in XTF format files in form of instantaneous amplitude, the standard from in which chirp-sonar data are saved by the system. In this way, geological interpretation of the seismic sections is favored, but phase information is lost. Data acquisition was performed by digital sampling of the seismic signal using the software SwanPro (Communication technology, Cesena) at a rate of 63 μ sec. All data were georeferenced with DGPS accuracy using geographic coordinates and the reference ellipsoid WGS84. The acquired dataset includes about 2300 km of seismic reflection lines homogeneously distributed within the lake surface (Fig. 2).

3.2. Seismic data processing

Seismic reflection profiles, acquired in XTF format, were subsequently converted to SEG-Y. Data processing and interpretation was carried out using the open package SeisPrho (Gasperini and Stanghellini, 2009). First, data were corrected for positioning and acquisition errors. Subsequently, they were filtered and edited for residual statics due to vertical movements generated by waves, with the final aim of obtaining high quality seismic reflection profiles suitable for interpretation. Because all acquisition parameters were kept constant during acquisition, it was possible to estimate the lake floor reflectivity at each ping by using a SeisPrho semi-automatic procedure, which also allowed for spherical divergence correction. Reflectivity and depth data were stored in ASCII space-separated files (i.e., in the SeisPrho REF format). At the end of the processing phase, a georeferenced bitmap (BMP) image and associated positioning file were generated for each seismic profile. After analysis of the entire dataset, a prominent reflector (H1), characterized by high amplitude and lateral continuity was detected and correlated over the entire basin (Fig. 3).

Taking advantage from our close-spaced grid of seismic reflection profiles, we used pseudo-3D techniques to determine lateral changes in the acoustic facies of the sedimentary sequence. We produced “flattened” versions of the seismic sections by using a special function of SeisPrho, which consisted in time-shifting the lake floor reflector (and the entire seismogram), to a horizontal reference level, 0 msec in our case, at each shot point (Fig. 3). In this way, a new set of “flattened” SEG-Y files, was created and subsequently sampled by using the SeisPrho *Time Slice* function, which allows for integrating seismic amplitudes within a time window (between 0 and 5 msec.) considered representative of the shallower sedimentary sequence around H1. The cumulative amplitude value determined at each shot by using this procedure was employed as an estimate of the degree of lateral coherence of internal reflectors at any given point, taking advantage by the data representation in form of instantaneous amplitude (only positive value). In such case, we assumed that well layered beddings were giving higher values of this coefficient relative to blind or chaotic deposits. Data derived in this way at each shot point were subsequently gridded to pro-

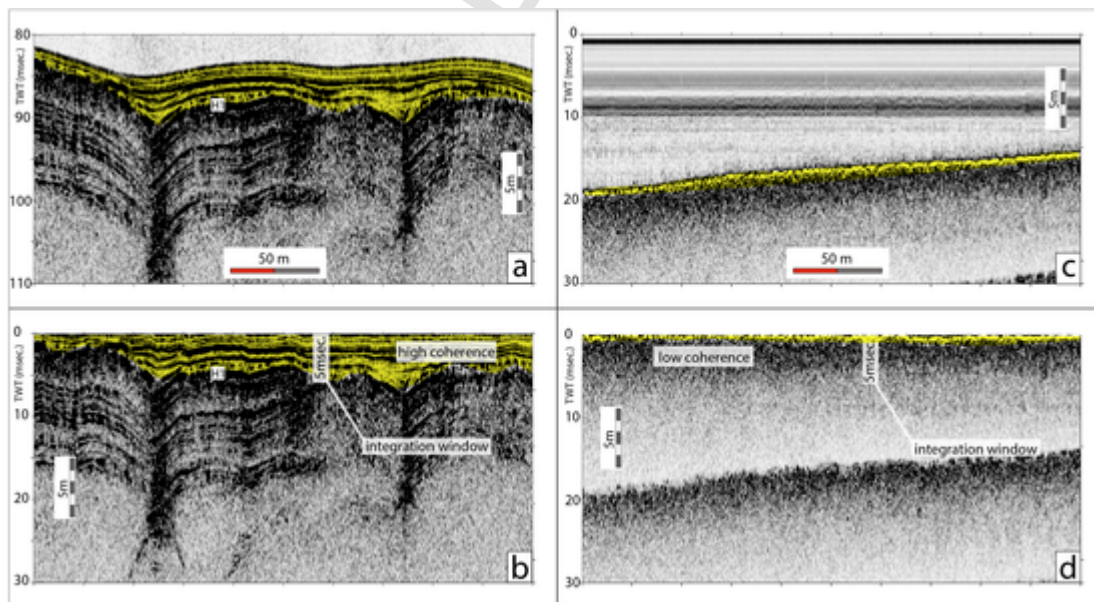


Fig. 3. Examples of seismic profiles from different sectors of the lake before (Top) and after (Bottom) flattening. Seismic unit (U1) above H1 is highlighted in yellow. The TWT window used to estimate reflector coherence (integration window) is also indicated. (For interpretation of the references to colour in this figure legend, the reader is referred to the web version of this article.)

duce what we have called a reflector *Coherency Map*. We note that well-layered seismic *facies*, encompassing alternate levels of finer and coarser grained deposits give the maximum values of coherence, while “blind” or “transparent” *facies*, due to the presence of chaotic sediments, gas, or homogeneous levels without internal reflectors correspond to minima of lateral coherence. However, this has been not considered a univocal parameter to define the seismic *facies*, and we used the reflector *Coherence Map*, in conjunction with other proxies (e.g., reflectivity), and performed our interpretation after ground-thruting plan view patterns on map with seismic sections.

3.3. Compilation of maps

Each map presented in this work was compiled using the Generic Mapping Tool (GMT) software (Wessel and Smith, 1998). After filtering and editing the georeferenced points (bathymetry, reflectivity amplitude, etc.), data were gridded using the *nearest-neighbors* algorithm of the GMT package. In this way, four *Netcdf* grids were produced: i) the lake floor bathymetry surface; ii) the H1 surface topography; iii) the reflectivity at the lake floor; iv) the reflector coherence. These grids allowed for compilation of thematic maps, including the thickness of U1, the sedimentary units resting on top of the H1 derived by subtracting the lake floor and the U1 surfaces. We used the average sound speed value of 1446 m/s, derived by measures in water column for depth-converting the bathymetry, and a value of 1500 m/s for a rough estimate of U1 thickness. All data were referenced to the datum of 64.527 m above sea level, the average lake level during the survey.

4. Results and discussion

4.1. Morphobathymetry and reflectivity of the lake floor

Fig. 4 displays the new morphobathymetric map of Lake Garda compiled after picking and gridding the lake-floor reflector of our dataset, and under assumptions and errors discussed in the “Methods” section. The morphological depression occupied by Lake Garda can be divided into two separate sub-basins: i) a northern deeper and narrow trough (we call it the *Axial Valley*) elongated in the NE-SW direction, reaching maximum depth of over −340 m relative to the datum (over 276 m below mean sea level); and ii) a shallower, broader and relatively flat area in the SE sector showing average depths above −100 m. The lake floor shows a rough and complex morphology in the southern axial sectors, while the maximum topographic gradients are reached along the western and eastern shores of the northern valley (Fig. 4). This bimodal distribution in the lake-floor morphology also affects the reflectivity pattern (Fig. 5), where the shallower and flat SE sector shows higher reflectivity, indicating coarser average grain-size or the presence of more consolidated deposits. Higher levels of reflectivity are also detected in the southern *Axial Valley* and along the lake shores.

Although several variables could affect propagation and scattering of acoustic wave at or near the lake-floor, experimental measurements of compressional wave attenuation (Shumway, 1960) as well as documented case studies (Gasperini, 2005) suggest that the single most important geotechnical property related to acoustic attenuation is the mean grain-size of the insonified sediment. In our case, the higher reflectivity values along the shorelines are related to the higher wave energies sorting out the finer particles, while high reflectivity anomalies recorded in the SW part of the lake (Fig. 5), suggest the presence of coarser sediments relative to other sectors. This observation suggests that either this sector is undersupplied by the fine-grained inflows deposits, or alternatively, it is kept clean by relatively strong bottom currents. Erosional scars disposed radially relative to the main SW-NE lake axis, both in the morphobathymetry and reflectivity maps (Figs. 4 and 5), point to the first hypothesis, since the radial erosions can be interpreted as relics of the glacial phase not yet obliterated by the onset of

the lacustrine sedimentation and/or strong bottom currents. We also note that both the eastern and the western coasts of the northern *Axial Valley* are punctuated by high reflectivity spots in correspondence river outflows (Fig. 5), which mark the presence of small wedges of coarser deposits.

4.2. Seismostratigraphy

The closely spaced grid of high-resolution seismic reflection profiles penetrating the upper tens of meters within the sedimentary sequence, enabled us to perform a seismo-stratigraphic analysis of recentmost Lake Garda sequence. We used as a reference the prominent H1 reflector (Fig. 3), characterized by high amplitude and lateral continuity. Although it shows variable characters in different sectors, H1 was correlated throughout the entire lacustrine basin. It marks, in fact, a sharp change in the seismo-stratigraphy, probably reflecting a diversity of geologic processes which shaped the Lake Garda basin starting from the LGM, when it was occupied by a major glacial tongue (Monegato et al., 2017 and references therein). These include incipient tectonic deformation at the southern front of the Alpine Chain, along the Giudicarie tectonic line (Fig. 1), associated with mass-wasting and gravitational instability, most probably related to the occurrence of strong earthquakes ($M_w > 6.0$), as also observed in other Alpine lakes (Fanetti et al., 2008; Lauterbach et al., 2012; Kremer et al., 2020).

Thus, the seismic unit between the lake floor and H1 (U1) marks a major change in the paleo-environmental conditions of the basin. Seismic *facies* and geometries within U1 show a great variability among different sectors, that were classified in five main seismic *facies* types, as diagnostic of different depositional environments.

- 1) *High-reflectivity facies* (Fig. 6a), characterized by a high reflectivity top and poor penetration of the seismic signal within U1. High-frequency seismic sources generally penetrate fine-grained units (silt-clay). Homogeneous and massive lithologies close to the shores, highlight the presence of coarse-grained sediments (sand or gravel) or early diagenesis horizons.
- 2) *Blind-gassy facies* (Fig. 6b), i.e., poor penetration or blanketing of seismic signal due to the presence of gas in the sediments (seismic “turbidity”), found in several sectors of the lake within U1. Gas is common in lake basins sediments, where sedimentary intakes are often associated with a large amount of organic substance. In sectors showing these *facies*, it was often impossible to accurately identify the base of U1, that was reconstructed by interpolating adjacent gas-free deposits.
- 3) *Plane-parallel bedding* (Fig. 6c). This pattern is common in areas where the stratigraphic succession appears undisturbed, leading to a continuous conformable layering. These *facies* are detected over wide sectors of the lake, particularly in the axial depocenters, where seismic reflectors mark sharp transitions from finer to coarser sediment beds. Typical patterns are marked by draping of fine-grained deposits conformable with the pre-existing topography or accreted as sub-horizontal tabular beds with onlap terminations, suggesting vertical or lateral deposition, respectively, poorly or not affected by local deformation. They include homogenite and turbidite beds.
- 4) *Hummocky facies*, (Fig. 6d), or deposits characterized by complex unconformable geometries shaped by density currents or by glacial debris deposited by collapsing debris-covered glaciers. Unit U1 shows locally significant variations in thickness and internal geometries that could probably be referred to reworking due to bottom currents. This is confirmed by internal undulations, particularly evident near the lake slopes or adjacent to morphological highs, similar to contourites (Rebesco and Stow, 2001).
- 5) *Deformed or chaotic facies* (Fig. 6e). In some sectors of the lake, pervasive deformations of the sediments are probably due to tectonics,

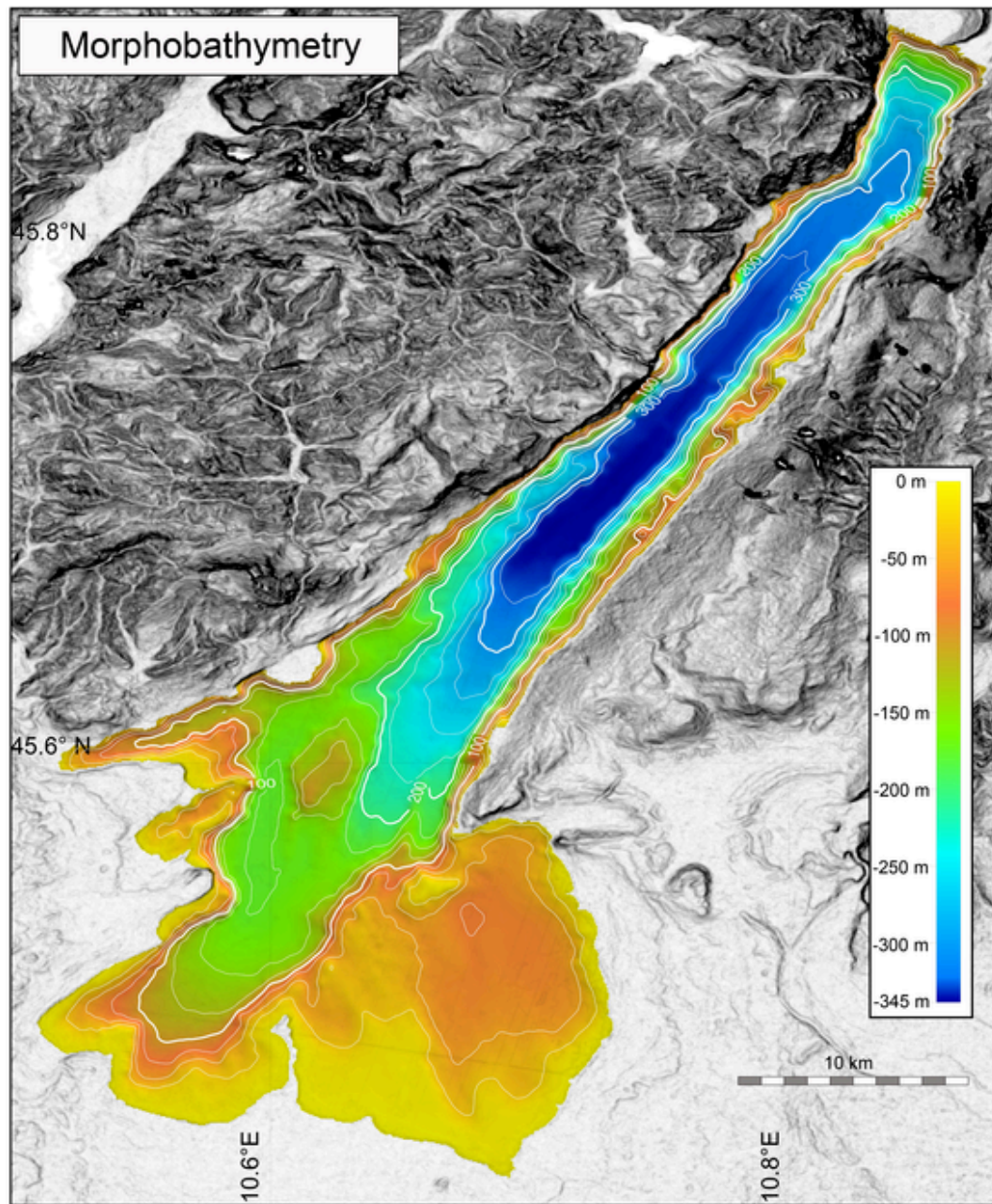


Fig. 4. Shaded-relief morpho-bathymetric map of Lake Garda compiled using the 2017 chirp-sonar dataset. We note that the southern, wider sector of the lake is characterized by a complex morphology, while the northern Garda (N of 45°36') is constituted by a rectilinear U-shaped trough SW-NE oriented, where maximum depths, and bathymetric gradients are reached.

gravity instability, gas and fluid migration, driving the formation of vertical fluid paths and mud diapirism. Given the shallow penetration of the seismic signal, it is not always possible to establish the nature of the deformations, i.e., whether they are or not related to deep-seated structures. All these processes could be interrelated, because their effects in the sedimentary sequence are clustered in key sectors of the basin, where most of the tectonic deformations correlate with structures observed onshore. From point to point, based on a combined analysis of maps and seismic profiles, we attempted a rough classification of different processes that likely produced the observed features (see next section).

4.3. Sediment thickness

Fig. 7 displays the map of unit U1 thickness derived from picking and correlation of reflector H1 throughout the entire lake surface. The northernmost stratigraphic body is a sediment wedge connected to the River Sarca, which starts to thicken towards the south and reaches its maximum thickness in the center of the *Axial Valley*, in correspondence of the lake depocenter, as displayed by the morphobathymetric map of Fig. 4. South of the depocenter, the thickness of U1 decreases abruptly, and remains rather constant throughout the southwestern basin, although very “patchy”. While in the northern part of the *Axial Valley* the sediment wedge corresponding to U1 appears tabular in shape, towards the south it shows a more irregular pattern, suggesting different deposi-

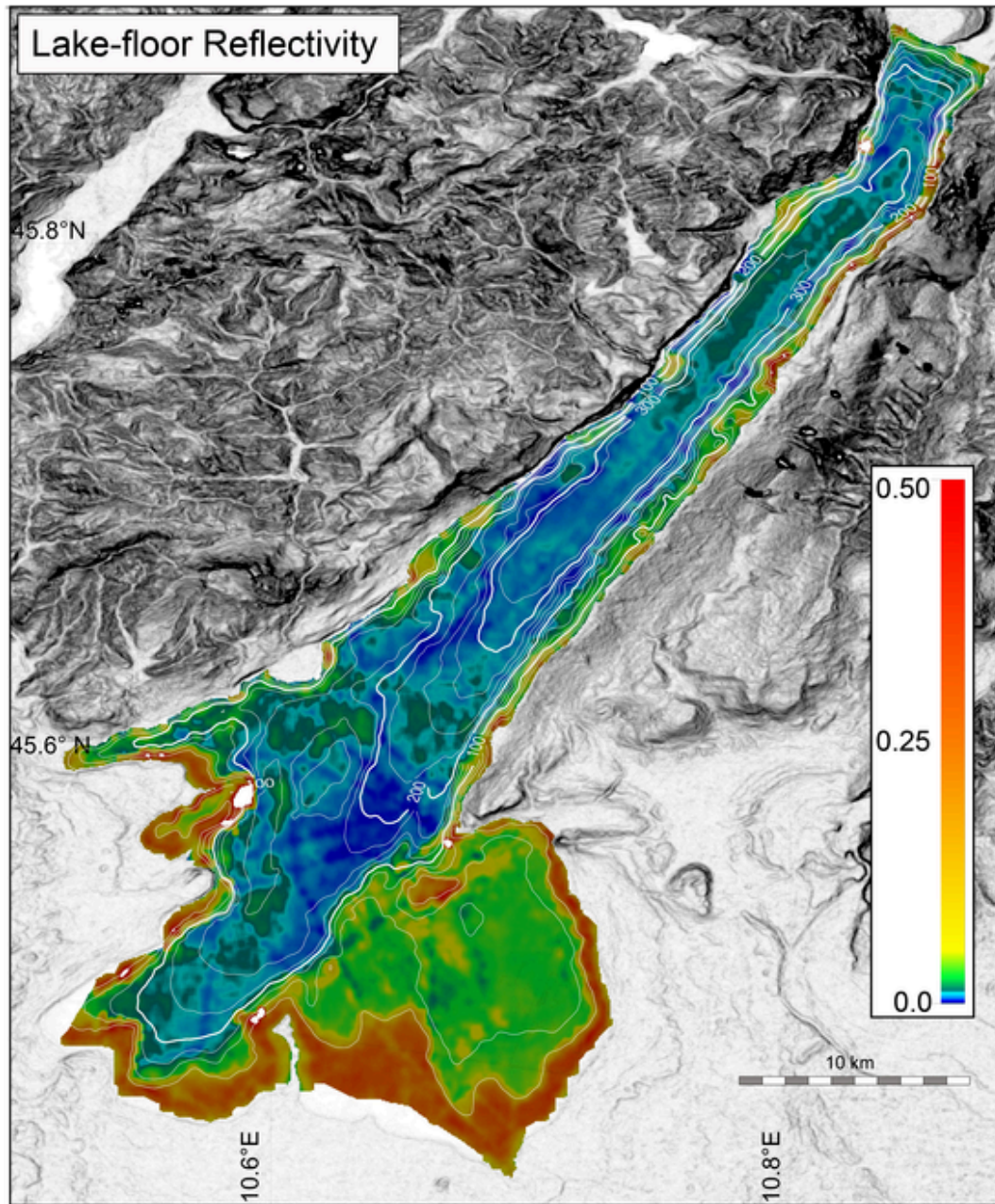


Fig. 5. Lake floor reflectivity map obtained from processing of seismic reflection profiles collected during the 2017 survey. We note the differences in average reflectivity between the axial valley and the wide southern shallow embayment, the former showing lower reflectivity patterns locally interrupted by more reflective bodies, mostly close to the shores and in correspondence of stream inflows.

tion mechanisms, sediment sources and/or post depositional deformation. This irregular pattern is also evident in the reflectivity map of the lake floor (Fig. 5). The SE shallower basin, also displays an irregular pattern, where the most evident feature is represented by an amphitheater-like ridge bounding the western lake shore, resembling the shape of the moraine hills onshore (Fig. 7). This suggests that sediment deposition might be driven by ice-melting, with U1 marking the glacier retreat. It is worthwhile noting that the lake floor reflectivity (Fig. 5) does not show this pattern, as it should if moraine deposits, characterized by higher reflectivity, were outcropping the lake floor. The differences between morphobathymetric and reflectivity maps indicate that glacial morphologies are generally draped by fine-grained lacustrine deposits.

4.4. Distribution of seismic facies

Analysis of the reflector's lateral coherence (Fig. 8) highlights differences between well-layered and chaotic/massive *facies*, and suggests the existence of different domains in the Lake Garda basin, characterized by a variety of geologic processes shaping the sedimentary sequence and the lake-floor morphology.

Based on the stratigraphic coherence map (Fig. 8), and also considering all available data, we compiled a map which highlights the distribution of seismic *facies* in different sectors, also including major structural and morphological elements (Fig. 9).

Fig. 9 map shows that the River Sarca sedimentary wedge is overlapped or inter-fingered in its northern part by sediment wedges from

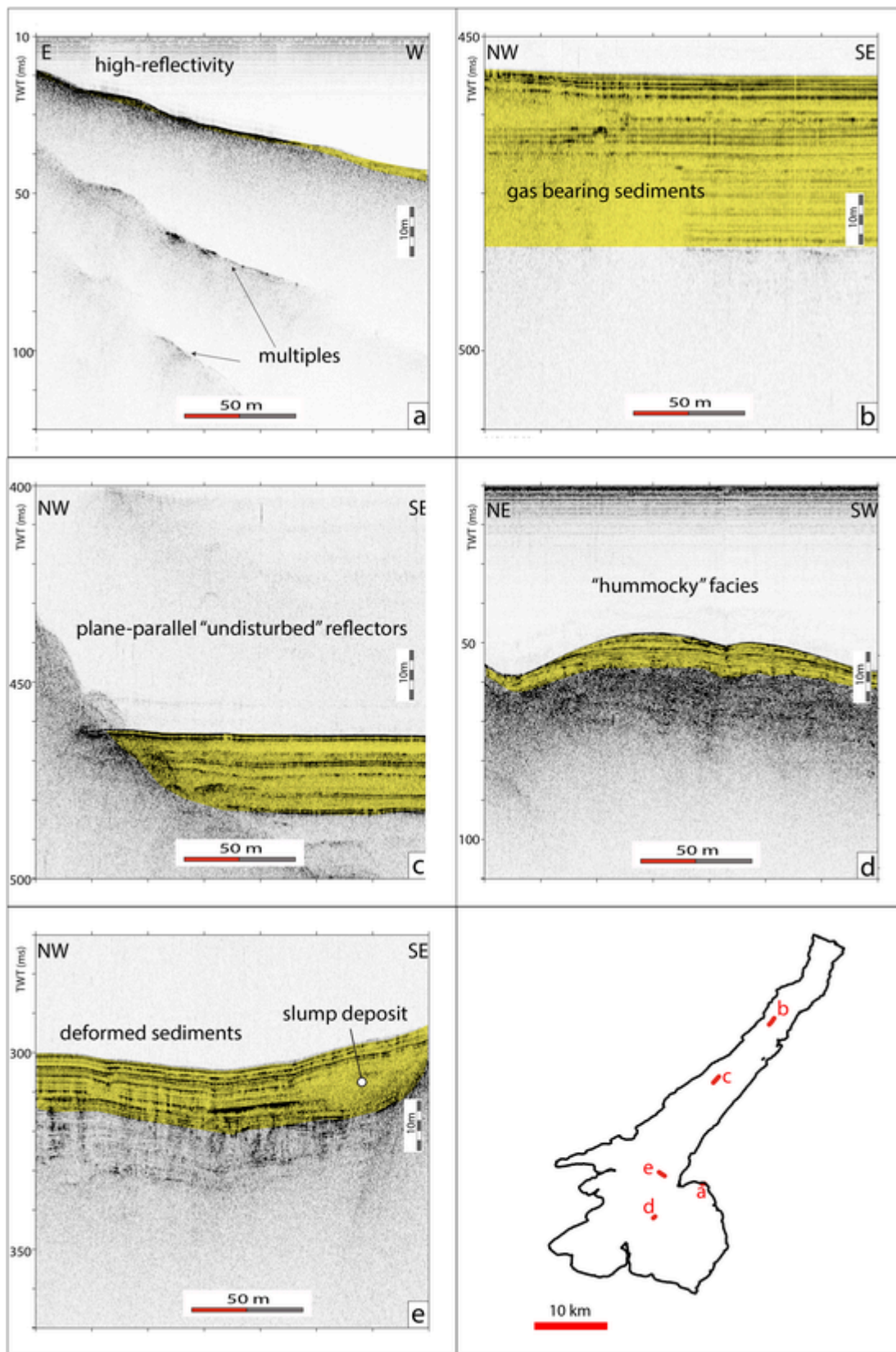


Fig. 6. Different seismic facies from different sectors of the lake, as diagnostic of prevailing geologic processes. a) high reflectivity with poor penetration; b) "blind" windows due to the presence of gas in the sediments; c) undisturbed bedding; d) hummocky facies; e) deformed or chaotic deposits.

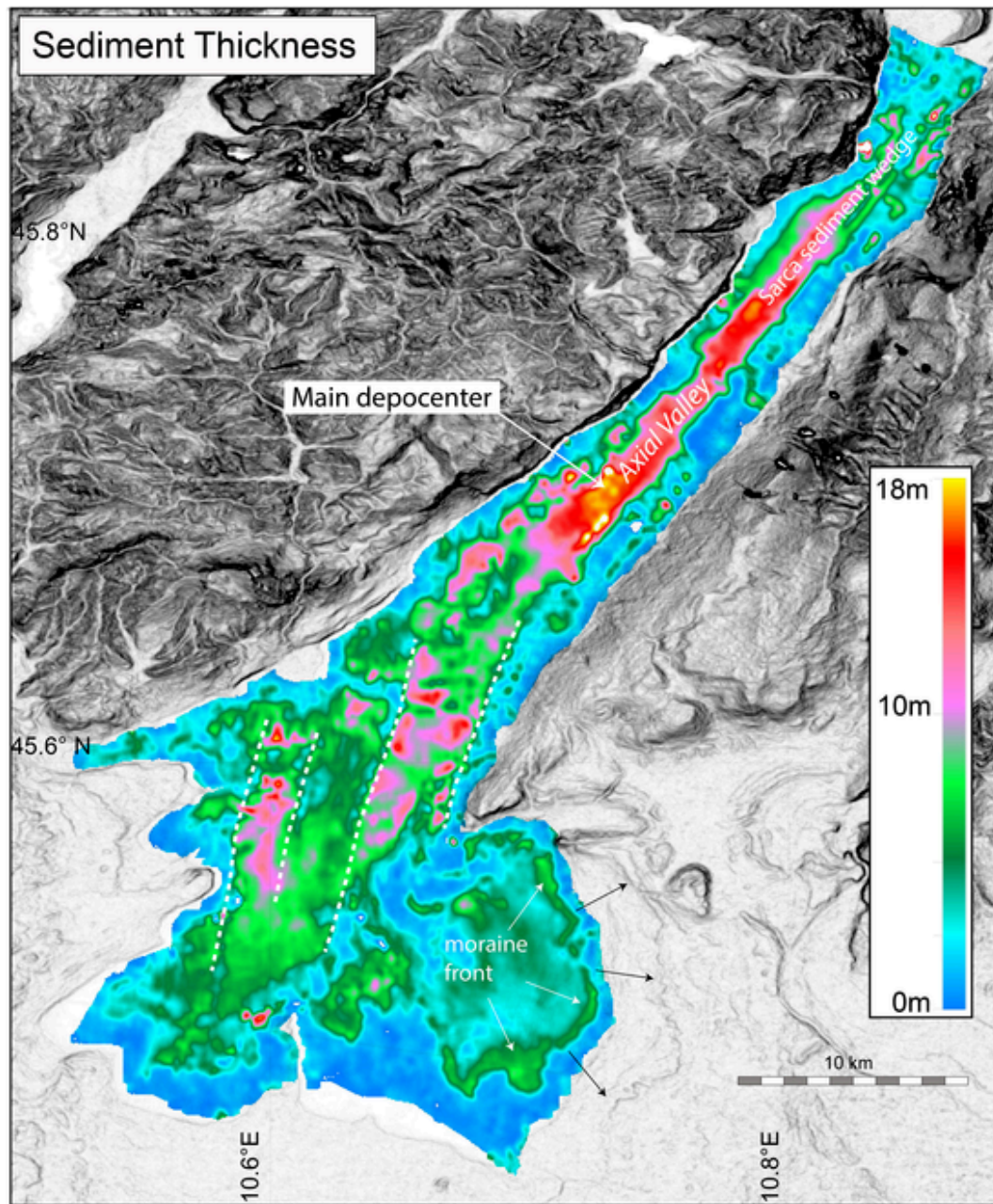


Fig. 7. Thickness of seismic unit U1. We note: -the sediment wedge of the River Sarca reaching up to the lake center and decreasing in thickness in the southern areas; -a system of transverse features (white dashed lines) separating sectors characterized by different thickness, probably controlled by tectonic structures at depth; -a moraine front, parallel to similar morphological feature observed onshore in the slope topographic map, probably formed during the latest retreat of the Lake Garda glacier after the LGM.

local streams, as also seen in the reflectivity map (Fig. 5). The River Sarca wedge is mostly constituted in its northern part by the *blind-gassy facies* (*facies b*, Fig. 6), and by plane-parallel bedding towards the south (*facies c*), up to the lake center. In the northern part, internal geometries of this body are barely imaged by our seismic dataset, due to the presence of high reflectivity horizons close to the river mouth, and of gas-bearing sediments inhibiting seismic penetration (Fig. 10).

We note that gas and fluids in the sediments are also present in the southern Sarca wedge, where they trigger the formation of mud diapirs intruding the sedimentary sequence, locally reaching up to the lake floor (Fig. 11).

The southern portion of the *Axial Valley* is characterized by pervasive deformations, either tectonic and/or gravitative (deformed or chaotic *facies*, Fig. 6e). These deformations are widespread to the

south of the *Axial Valley*, where they alternate with plane-parallel bedding.

The *hummocky facies* (Fig. 6d), typical of sediments affected by bottom current reworking, are widespread in the entire basin, particularly in correspondence of steep slopes, where the erosional effect is enhanced by increased velocities of the water flow.

The *Axial Valley* shows the deepest bathymetries (Fig. 3) and largest thicknesses of U1 (Fig. 7), as well as the lowest value of lake floor reflectivity (Fig. 5). This suggests that most of the sediments supplied by River Sarca and by the several minor streams on both the E and W shores, find here their final sink. The greater depths and the larger accommodations are probably inherited by more efficient glacial carving in the central part of the glacial tongue, or, alternatively could be tectonically controlled, although our shallow-penetrating data do

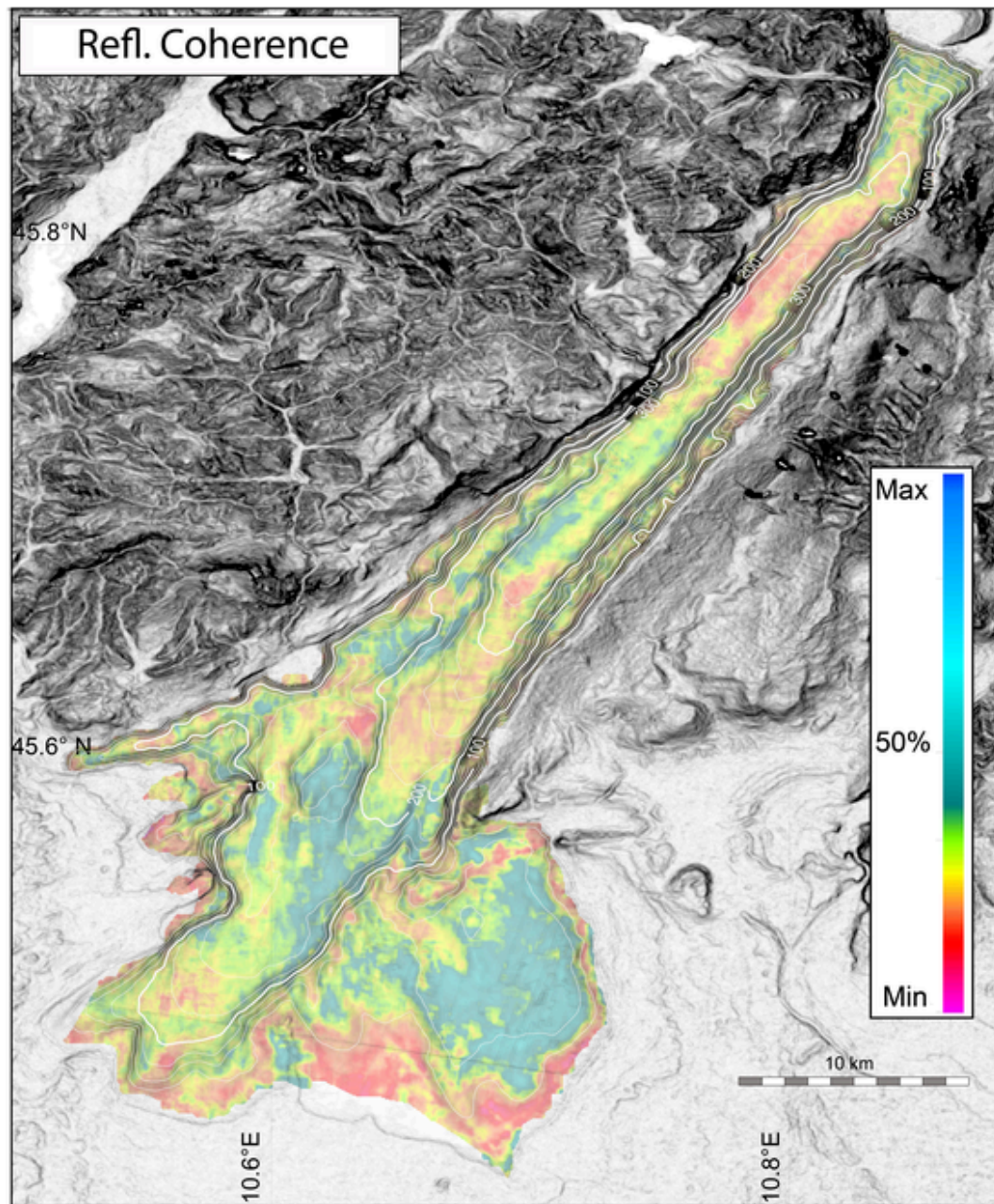


Fig. 8. Map of the stratigraphic coherence (see methods for details) superimposed to the slope map of the bathymetry. This representation led us to distinguish between well-layered vs chaotic or not penetrated deposits. It was used as a base for the morpho-structural maps presented in Fig. 9.

not help in discriminating between these effects. High-reflectivity spots punctuating the shores in this region indicate relatively coarse grain sizes in correspondence of the main supplies or distributed along the coasts. In the axial depocenter, the plane parallel undisturbed bedding prevails, although from point to point we could observe undulations (*hummocky facies*), probably due to reworking by density and/or hyperpycnal currents descending from the N. This is particularly visible in the U1 thickness map (Fig. 7), where flat tabular beds alternate with undulated sedimentary bodies. *Gassy facies* are also present, although less extensively than in the southern sectors.

The south-western basin is also influenced by the sediment supply of the tributaries, but in this sector we can observe more complex geometries. Seismic profiles evidence in this area the presence of chaotic massive bodies, forming lenses interbedded in the well layered

deposits (Fig. 12), alternating with undulated and folded sediments in correspondence of compressive tectonic structures.

The south-eastern shallow embayment shows peculiar morphological features associated with the limited thickness of U1. This sector is separated from the *Axial Valley* by a morphological step, developing along a regional tectonic structure, the *San Vigilio-Sirmione-Rivoltella* fault (SSR, in Berlusconi et al., 2013) parallel to the eastern lake shore (Fig. 9). This topographic sill marks a sharp boundary between the two sub-basins, separated by over 100 m of vertical offset (Fig. 4). The presence of this sill probably inhibits the supply of fine-grained sediments from the north, along *Axial Valley* by bottom density currents. As a consequence, seismic reflection profiles located in the south-eastern sub-basin display a limited thickness of U1 and higher lake floor reflectivity, due to coarser sediments and glacial morphology only partially draped by more recent deposits (Fig. 7).

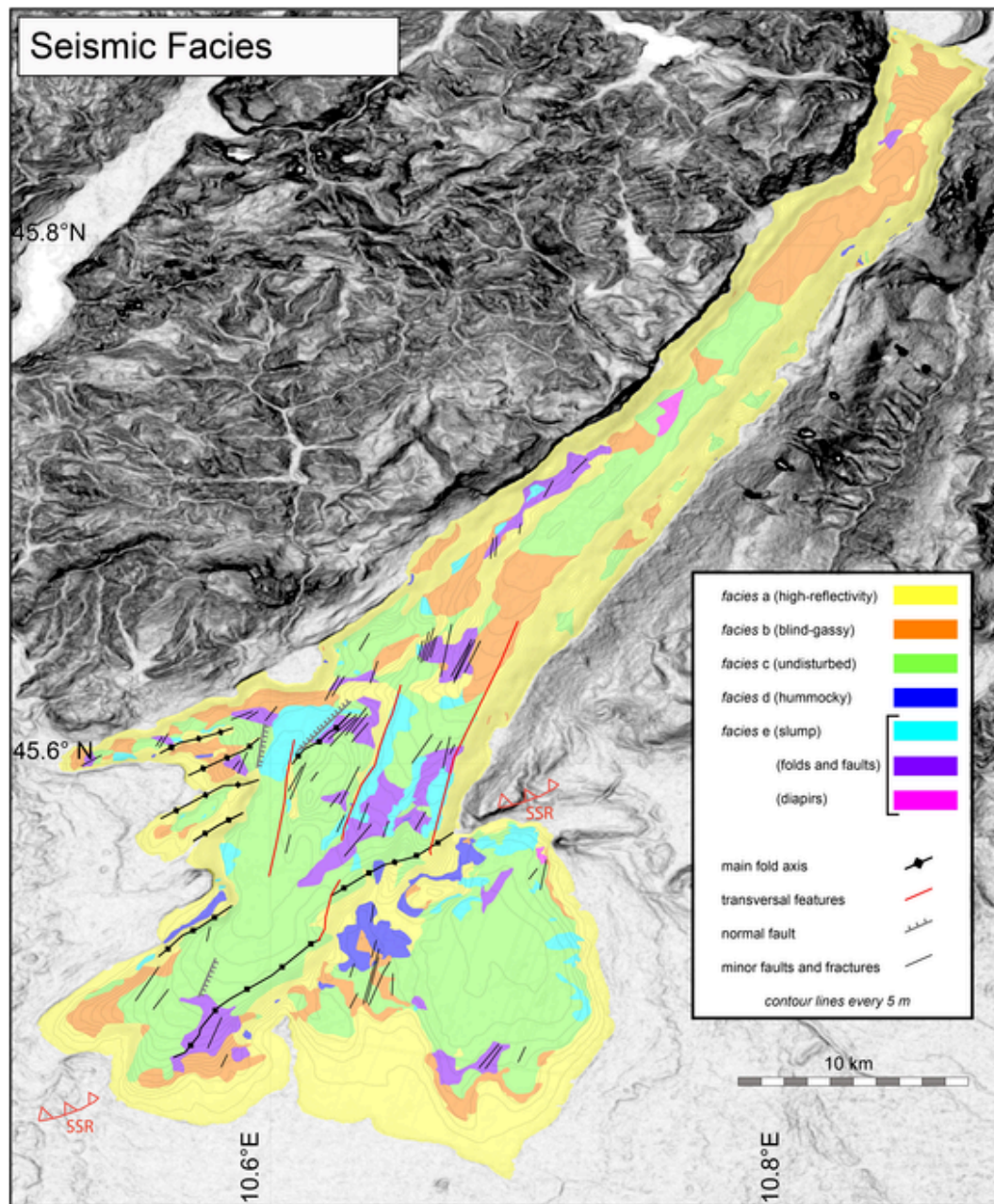


Fig. 9. Seismic facies distribution and main morpho-tectonic elements (see legend) based on analysis of seismic images and all available data. Position of San Vigilio-Sirmione-Rivoltella (SSR) fault close to the lake shores (sawteeth red lines) is from Berlusconi et al. (2013). (For interpretation of the references to colour in this figure legend, the reader is referred to the web version of this article.)

4.5. Morpho-tectonic analysis

Although our seismic profiles penetrate only few tens of meters in the sedimentary sequence, we note that the folded units in the southern sector of the basin show a NE-SW orientations, parallel to the fold-related faults described in the literature (e.g., Curzi et al., 1992; Berlusconi et al., 2013). Moreover, gravitative deposits which punctuate the southern *Axial Valley* are clustered in areas close to, or corresponding with, the presence of active tectonic features. Interpretation of seismic reflection profiles and compiled maps could be summarized in the sketch displayed in Fig. 9, which includes different domains, characterized by different geologic processes: i) the River Sarca inflow, from the northern shore with high reflectivity and gas-bearing sedi-

ments dispersed along the Axial Valley and onlapping the steep slopes; ii) the axial depocenters, which develops along the NE-SW oriented valley showing flat top and plane parallel bedding; iii) the SW sector, affected by active tectonic deformations, and slumps; iv) the SE basin, to the east of a bathymetric scarp oriented SW-NE, which separates the main valley by a wide shallow embayment showing minimum average depths.

The morphological feature separating the *Axial Valley* from the southeastern shallow embayment coincides with the *San Vigilio-Sirmione-Rivoltella* (SSR) fault, that has been studied onshore by numerous authors (Cozzaglio, 1933; Piccoli, 1965; Carraro et al., 1970; Sauro, 1974; Semenza, 1974; Castellarin, 1982; Panizza et al., 1981; Cavallin et al., 1984). The SSR fault appears the most prominent of a complex compressional pattern affecting the southern sectors

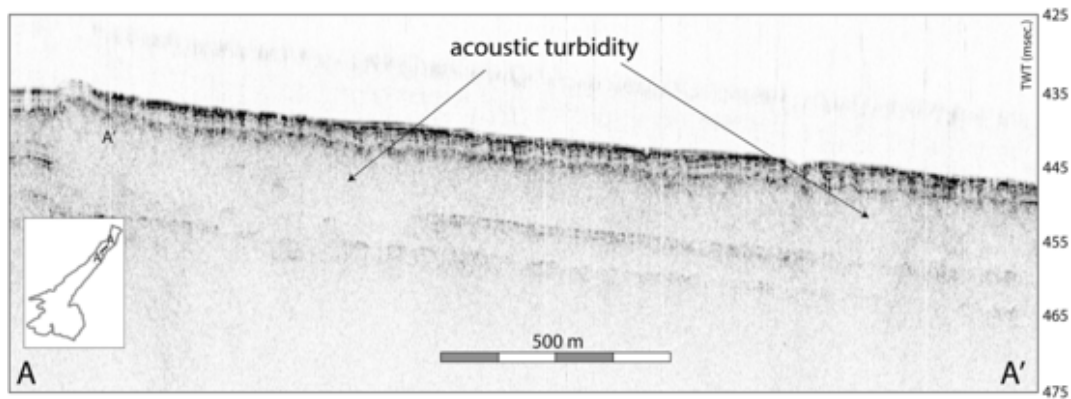


Fig. 10. Portion of seismic reflection profile from the northern Axial Valley, in an area showing low penetration of the seismic signal that could be due to the combined effect of gas in the sediments (acoustic turbidity *sensu* Hovland and Judd, 1988) and/or to relative coarse-grained sediments carried by the rivers.

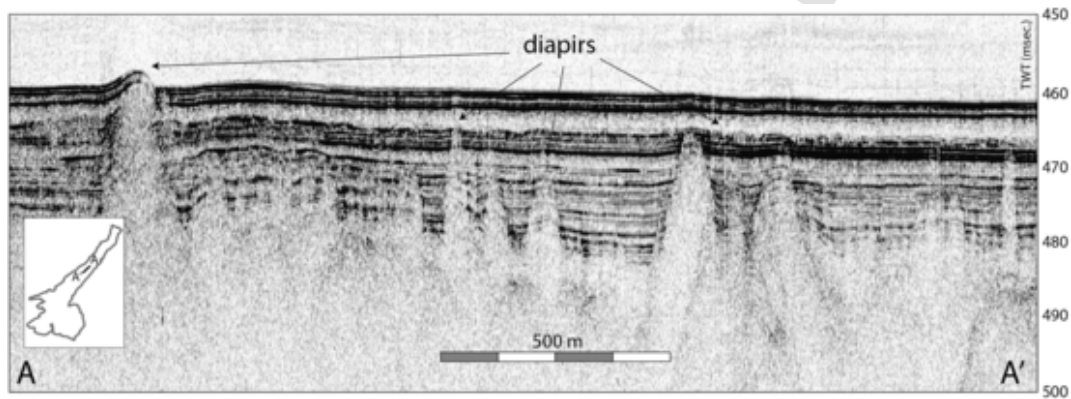


Fig. 11. Portion of seismic reflection profile from the northern Axial Valley, in an area showing good penetration of the seismic signal. We note the widespread presence of intrusions in the well-layered sedimentary sequence, interpreted as mud diapirs which locally reach up to the lake floor.

of the lake floor (Figs. 9 and 12). Orientation and nature of such deformations fit well with structural and neotectonics evidence reported onshore (Sauro, 1974; Baroni, 1985, 1990, 2010, 2017; Galadini and Galli, 1999; Sauro and Zampieri, 2001; Galadini et al., 2001; Berlusconi et al., 2013). Even the leakage of fluids and the widespread mud diapirism visible in many sectors of the lake (Fig. 11), are possibly related to seismicity and seismic shaking, as observed in similar contexts, where fluid-related features seems to play an important role in seismogenesis and sediments deformation (Gasperini et al., 2012, 2018, 2020; Lazar et al., 2019; Haddad et al., 2020).

The western sector of Lake Garda is characterized by the most intense tectonic deformations, also evidenced by the complexity of the shoreline showing the presence of structurally-controlled narrow gulfs (Fig. 2). Short amplitude folds (Fig. 12) align with the NW-SE trending regional thrusts, along the South Giudicarie tectonic line (Fig. 1), and rotate clockwise towards the south in correspondence of the southern Garda basin (Castellarin, 1982; Cremaschi, 1987). This system also includes the northern sector of the Sirmione peninsula (Fig. 2), and continues towards the south of Lake Garda, beneath the Po plain sediments (Pieri and Groppi, 1981). In our maps, compressive fronts appear dissected by NNE-SSE oriented transverse features, mostly evident in the lake-floor morphology (Fig. 4) and U1 thickness (Fig. 7). These transverse lines could be morphological scars associated to LGM phase, or could be due to tectonic deformations, accommodating the rotation of compressive fronts towards the south, as also observed onshore (Castellarin, 1982; Serva, 1990; Galadini et al., 2001).

4.6. Stratigraphic correlations

Stratigraphic studies of the post LGM sedimentary sequence are poor.

An exception is represented by a study focused on concentration of chemical pollutants at the water-sediment interface and within the first meter of sedimentary sequence (Bossi et al., 1992), carried out without geophysical constraints. Another, is represented by the work of Curzi et al. (1992), where a set of seismic reflection and refraction profiles collected from the lake floor, although less densely spaced, was discussed. In the study by Bossi et al. (1992), three sediment cores were collected in the southern Lake Garda basin. ^{137}Cs dating of the shallower sediment sequence (<1 m) enabled these authors to obtain accurate estimates of sedimentation rates in the 1963–1989 time-interval. Values obtained, in the order of 2 cm/y can be considered representative of the very upper part of the sequence only, i.e., less than a century before present. They appear to be overestimated at the scale of 10 ka, also considering the effects of compaction. In fact, based on these values we should assume an unrealistic thickness of hundreds of meters for the Holocene deposits. Onshore-offshore correlation of glacial/fluvioglacial deposits dating at the end of LGM (Berlusconi et al., 2013), carried out on seismostratigraphic observations (Curzi et al., 1992), could be used to constraint the thickness of lacustrine deposits. We note that, in Berlusconi et al. (2013) reconstruction, the unconformity marked as base of “lacustrine deposits” (the top-most unit) coincides with our U1. If we assume this correlation valid, H1 should mark the onset of lacustrine condition after the LGM, dating back to after 17.46 ± 0.2 ka cal BP according to Ravazzi et al.

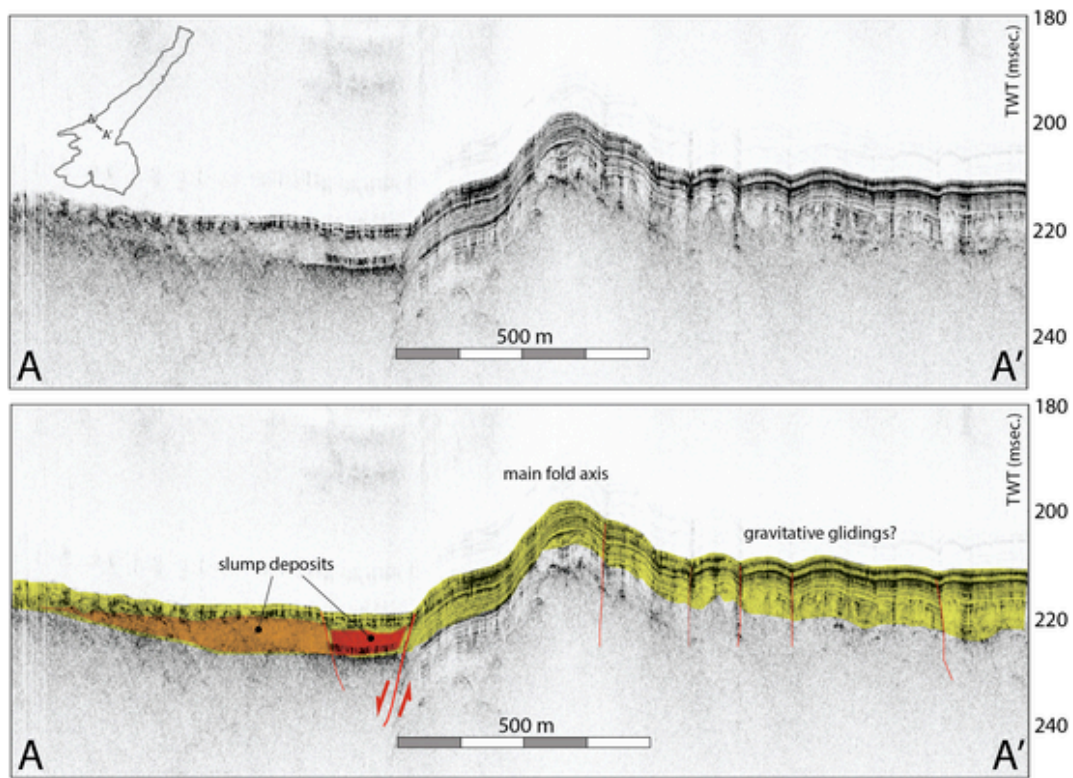


Fig. 12. Segment of seismic reflection profile crossing NW-SE the southern Axial Valley showing incipient deformation of the sediment and the presence of slump deposits interlayered in the plane-parallel bedding.

(2014). This implies a maximum deposition rate around 1.2 mm/y, a value that, although reasonable, should be verified by further stratigraphic analyses. On the other side, this rough estimate is coherent with the assumption of H1 marking the (probably complex) onset of lacustrine environment after the LGM. We note that the character of U1 changes markedly going from the southern to the northern lake's sectors. In particular, observation that the moraine amphitheater-like feature observed in the U1 thickness map witnesses its stratigraphic correlation to the glacial phase. In this way, we can identify at least two main sectors of different age along the lake axis: the first sector external to the moraine ridge, older than ca 17 ka, and a second internal, towards north-northwest. According to the literature, the glacial retreat was very fast after a preliminary phase of glacial collapse, at its outer border (Ravazzi et al., 2014; Baroni, 2017; Monegato et al.,

2017). This phase, according to Ravazzi et al. (2014), is older than 17 ka, and is well constrained by complex glacio-lacustrine deposits bounding the southern border of the lake which predate 16 ka (Baroni, 2017). We could then assume that H1 is diachronic, recording subsequent stages of the glacier collapse which should have occurred in different times along the lake's axis.

4.7. Megaturbidite-homogenite beds

In the lake center, along the Axial Valley, U1 shows its maximum thickness and is composed of plane-parallel layers (Fig. 13). Here, two major transparent units are observed below the lake floor, both characterized by a homogeneous/transparent facies resting on a highly reflective basal unit. Following stratigraphic analysis carried out in similar

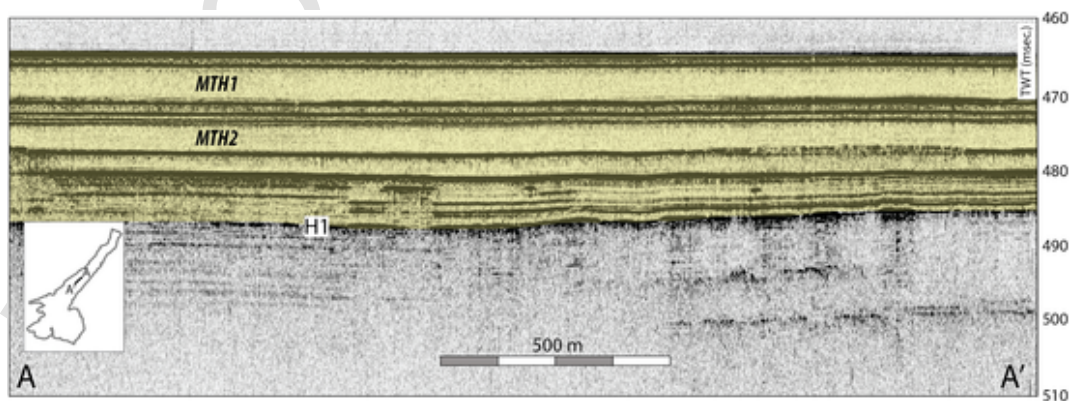


Fig. 13. Seismic profile GA627 along the Axial Valley in the lake center. U1, above reflector H1 is marked in yellow. We note the presence of two peculiar layers, MTH1 and MTH2 in the stratigraphic sequence. They are marked by highly reflective beds, and show a transparent facies, indicating homogeneous, fine-grained lithologies. According to similar examples studied in deep-sea basin and lakes (see text) we interpret these units as megaturbidite-homogenite beds, probably deposited after high energy events. (For interpretation of the references to colour in this figure legend, the reader is referred to the web version of this article.)

environments (Fanetti et al., 2008; Lauterbach et al., 2012) or in deep sea basins (Rothwell et al., 1998; Polonia et al., 2013, 2017; Kremer et al., 2020) we interpret such feature as megaturbidite-homogenite beds. In this interpretation, MTH1 and MTH2 (Fig. 13) mark major high energy events in the recent depositional history of the lake, probably encompassing the Holocene. The uppermost MTH1, is located at about 1.3 m below the lake floor, and shows a thickness of over 6 m. The deeper MTH2, is located at 6.8 m below the lake floor and shows a thickness of about 2.6 m. A third MTH beds is possibly located immediately below MTH2, with a maximum thickness of about 2 m, but its signature is less well defined relatively to the two units above. Although further data are needed, we suggest that these high energy deposits might have been triggered by major earthquakes in this seismically active region. Assuming the rate of 1.2 mm/y obtained by stratigraphic correlations of our seismo-stratigraphic data, we could speculate that at least MTH1 falls during historical times, about 1 ka before present or more. In such a case, several candidates are available as possible triggering mechanisms, including the 1117 and 1222 earthquakes. Similar lacustrine resedimented deposits (seismites) were described in Central Switzerland (Strasser et al., 2013), NW Alps (Chapron et al., 1999; Beck, 2009), as well as in Lake Como and Lake Iseo (Fanetti et al., 2008; Lauterbach et al., 2012). Following the same line of reasoning, the deeper MTH2 might be correlated with the surface faulting event occurred in the mid-III Century AD in the Adige Valley (Galadini and Galli, 1999). It is important to observe that megaturbidites do not necessarily indicate a seismic trigger, but can result from spontaneous delta collapses as well. A good example is the Tauredunum event in Lake Geneva (Kremer et al., 2012) or the megaturbidites in Lake Brienz (Girardclos et al., 2007). For this reason, further studies and the collection of gravity cores long enough to sample the MTH beds are needed to constraint emplacement age and triggering mechanisms of the observed resedimented deposits, which constitutes over 50% of the stratigraphic section in the Lake Garda depocenter. Such high energy events are relatively rare in the Lake Garda Holocene record, in line with long recurrence intervals for large-magnitude earthquakes in the region (Michetti et al., 2012; Berlusconi et al., 2013; Livio et al., 2014).

5. Conclusions

A new set of seismic reflection profiles collected in Lake Garda, the largest Italian lake located at the southern edge of the Alpine chain, allowed to study geologic processes at the scale of the last 10 ka, shaping its floor and the shallow substratum. We correlated and mapped a prominent reflector delimiting the base of a lacustrine sedimentary unit (H1) which, based on available stratigraphic information, records the complex and probably diachronic onset of lacustrine conditions after the Last Glacial Maximum (LGM). Since then, a number of processes have left their signatures in the stratigraphic sequence of the lake, such as the selective supply of sediment from major and minor river streams, and their redistribution by bottom currents; the effect of active tectonic deformations at the southern front of the Alpine orogenic belt; widespread gravity failures, mostly clustered in the southernmost basin, probably triggered by major historical earthquakes. The variable effect of such processes in different sectors of the basin was recognized analysing with different techniques the newly collected data. The most prominent sedimentary bodies observed in the lake depocenter were interpreted as two seismoturbidite-homogenite beds, probably correlated with major historical or proto-historical earthquakes. These deposits record the effect of two high-energy events, and encompass over 50% of the entire Holocene sequence, suggesting long recurrence periods for major earthquakes in this region (two events in 10 ka). Moreover, among other processes, the sediments of southern Lake Garda are clearly affected by incipient tectonic deformations. We conclude that the Lake Garda basin provides a unique opportunity to identify geody-

namics and related earthquake hazards at the southern front of the Alpine chain.

Uncited references

Declaration of competing interest

The authors declare no conflict of interests.

Acknowledgments

We thank the many people who helped in different ways during field campaign organization and execution. The list is long, but should include Erica Cabrioli, Michele Donatoni and Pierluigi Malavasi. Thanks to the staff of *Proambiente*, and in particular the director, Dr. Antonella Poggi, without whom this work would not have been possible. Suggestions and comments from the Editor, Carlo Baroni and an anonymous referee have greatly improved the quality of the paper. The project has been partly supported within the Project “Green Lake” by the *Fondazione Comunità Bresciana*.

Appendix A. Supplementary data

Supplementary data associated with this article can be found in the online version, at <https://doi.org/10.1016/j.geomorph.2020.107427>. These data include the Google map of the most important areas.

References

- Ammann, B., Birks, H., Walanus, A., Wasylukowa, K., 2013. Late glacial multidisciplinary studies. *Encyclopedia of Quaternary Science* 3, 2475–2486.
- Baroni, C., 1985. Note sulla paleogeografia olocenica della costa occidentale del Lago di Garda. *Geogr. Fis. Din. Quat.* 8, 49–61 (in Italian).
- Baroni, C., 1990. La frana di Salò. *Atti Ticinesi di Scienze della Terra* 33, 63–90 (in Italian).
- Baroni, C., 2010. Paleolivelli tardoglaciali e olocenici del Lago di Garda. In: Orombelli, G., Cassinis, G., Gaetani, M. (Eds.), *Una nuova geologia per la Lombardia. Convegno in onore di Maria Bianca Cita*, Milano 6–7 Novembre 2008, Istituto Lombardo Accademia di Scienze e Lettere. *Incontri di Studio*, 54, LED Edizioni Universitarie, Milano. pp. 231–254 (in Italian).
- Baroni, C. (2017). Lake Garda: an outstanding archive of Quaternary geomorphological evolution. In: Soldati M. and Marchetti M. (Eds), *Landscape and Landforms of Italy. World Geomorphological Landscapes* 169–179, Springer, ISBN: 978-3-319-26192-8, ISSN: 2213-2090, doi: 10.1007/978-3-319-26194-2_14.
- Beck, C., 2009. Late Quaternary lacustrine paleo-seismic archives in north-western Alps: examples of earthquake-origin assessment of sedimentary disturbances. *Earth Sci. Rev.* 96, 327–344. doi:10.1016/j.earscirev.2009.07.005.
- Berlusconi, A., Ferrario, M.F., Livio, F., Michetti, A.M., Violante, C., Esposito, E., Porfido, S., Fiaccavento, P., Ripamonti, L., Roncoroni, M., 2013. Quaternary faults and seismic hazard in the lake Garda area. *Ingegneria Sismica*, XXX 1–2, 10–35.
- Bini, A., Cita, M.B., Gaetani, M., 1978. Southern Alpine lakes - hypothesis of an erosional origin related to the Messinian entrenchment. *Mar. Geol.* 27 (3–4), 271–288.
- Bossi, R., Larsen, B., Premazzi, G., 1992. Polychlorinated biphenyl congeners and other chlorinated hydrocarbons in bottom sediment cores of Lake Garda (Italy). *Sci. Total Environ.* 121, 77–93.
- Calderoni, A., 2003. Monitoraggio della presenza di DDT e di altri contaminanti nell'ecosistema Lago Maggiore. In: *Rapporto Annuale Aprile 2002 – Maggio 2003. Internazionale per la protezione delle acque italo-svizzere*, Commissione (in Italian).
- Camassi, R., Rossi, A., Tertulliani, A., Pessina, V., Caracciolo, C.H., 2011. Il terremoto del 30 Ottobre 1901 e la sismicità del versante occidentale del Garda. *Quaderni di Geofisica* 88 36 pp. (in Italian). ISSN 1590-2595. <https://www.earth-prints.org/bitstream/2122/7478/1/quaderno88.pdf>.
- Carraro, F., Dal, Piaz, G., Sacchi, R., 1970. Serie di Valpelline e Il Zona Diorito-Kinzigitica sono i relitti di un ricoprimento proveniente dalla Zona Ivrea-Verbano. *Mem. Soc. Geol. Ital.* 9, 197–224 (in Italian).
- Castellarin, A. (1982). Lineamenti ancestrali sudalpini. In: Castellarin A., Vai G.B. (Eds.): *Guida alla Geologia del Sudalpino centro-orientale. Guide Geologiche Regionali*, Soc.Geol. It., pp. 41–55 (in Italian).
- Castellarin, A., Ferrari, A., 1972. Evoluzione paleotettonica sinsedimentaria del limite tra “Piazzaforte Veneta” e “Bacino lombardo” a nord di Riva del Garda. *Giorn. Geol.* 38, 11–212 (in Italian).
- Castellarin, A., Cantelli, L., Fesce, A.M., Mercier, J.L., Picotti, V., Pini, G.A., Prosser, G., Selli, L., 1992. Alpine compressional tectonics in the Southern Alps. Relationships with the N-Apennines. *Annales tectonicae* 6, 62–94.
- Castellarin, A., Vai, G.B., Cantelli, L., 2006. The Alpine evolution of the Southern Alps around the Giudicarie faults: a Late Cretaceous to Early Eocene transfer zone. *Tectonophysics* 414, 203–223.

- Cavallin, A., Giorgetti, F., Manfredini, U., Peverieri, P., 1984. Seismic hazard: computer elaboration in the Friuli region (Italy). In Abstracts: 27th International Geological Congress. IUGS 22.
- Chapron, E., Beck, C., Pourchet, M., Deconinck, J.-F., 1999. 1822 earthquake-triggered homogenite in Lake Le Bourget (NW Alps). *Terra Nova* 11, 86–92. doi:10.1046/j.1365-3121.1999.00230.x.
- Cozzaglio, A., 1933. Note illustrative della Carta Geologica d'Italia, Fogli 48 Peschiera e 62 Mantova. Uff. Idr. Magistr. Acque, Venezia 205 pp. (in Italian).
- Cremaschi, M., 1987. Paleosols and Vetusols in the Central Po Plain (Northern Italy): A Study in Quaternary Geology and Soil Development. UNICOPLI, Milano 306 pp. ISBN 884000081X.
- Cremaschi, M., 1994. Le Glacialisme Quaternaire de la Vallée de l'Adige. *Preistoria Alpina* 28, 285–290.
- Curzi, P.V., Castellarin, A., Ciabatti, M., Badolini, G., 1992. Caratteri morfostutturali sedimentologici e genetici del Lago di Garda. *Boll. Soc. Torricelliana Sci. Lett. Faenza* 43, 3–111.
- Doglioni, C., Bosellini, A., 1987. Eoalpine and mesoalpine tectonics in the Southern Alps. *Geol. Rundsch.* 76, 735–754.
- Fanetti, D., Anselmetti, F.S., Chapron, E., Sturm, M., Vezzoli, L., 2008. Megaturbidite deposits in the Holocene basin fill of Lake Como (southern Alps, Italy). *Palaeogeogr. Palaeoclimatol. Palaeoecol.* 259, 323–340.
- Fuganti, A., Bazzoli, G., Morteau, G., Valley, A., Nat, S.T.S., 2001. La genesi della Valle dell'Adige. *Acta Geologica* 77, 205–219 (in Italian).
- Galadini, F., Galli, P., 1999. Paleoseismology related to the displaced Roman archaeological remains at Egna (Adige valley, northern Italy). *Tectonophysics* 308, 171–191.
- Galadini, F., Galli, P., Cittadini, A., Giaccio, B., 2001. Late Quaternary fault movements in the Mt. Baldo-Lessini Mts. sector of the Southalpine area (northern Italy). *Geol. en Mijn. Neth. J. Geosci.* 80, 187–208.
- Galli, P., 2005. I terremoti del Gennaio 1117. Ipotesi di un epicentro nel cremonese. *Il Quaternario* 18, 87–100 (in Italian).
- Gasperini, L., 2005. Extremely shallow-water morphobathymetric surveys: the Valle Fattibello (Comacchio, Italy) test case. *Mar. Geophys. Res.* 26, 97–107.
- Gasperini, L., Stanghellini, G., 2009. SeisPrho: an interactive computer program for processing and interpretation of high-resolution seismic reflection profiles. *Comput. Geosci.* 35, 1497–1507.
- Gasperini, L., Polonia, A., Del Bianco, F., Etiope, G., Marinaro, G., Favali, P., Italiano, F., Çağatay, M.N., 2012. Gas seepage and seismogenic structures along the North Anatolian Fault in the eastern Sea of Marmara. *Geochem. Geophys. Geosyst.* 13 (10). doi:10.1029/2012GC004190.
- Gasperini, L., Polonia, A., Çağatay, M.N., 2018. Fluid flow, deformation rates and the submarine record of major earthquakes in the Sea of Marmara, along the North-Anatolian Fault system. *Deep-Sea Res. II Top. Stud. Oceanogr.* 153, 4–16.
- Gasperini, L., Lazar, M., Mazzini, A., Lupi, M., Haddad, A., Hensen, C., Schmidt, M., Caracausi, A., Ligi, M., Polonia, A., 2020. Neotectonics of the Sea of Galilee (Northeast Israel): implication for geodynamics and seismicity along the Dead Sea fault system. *Sci. Rep.* 10, 1–17.
- Girardclos, S., Schmidt, O.T., Sturm, M., Ariztegui, D., Pugin, A., Anselmetti, F.S., 2007. The 1996 AD delta collapse and large turbidite in Lake Brienz. *Mar. Geol.* 241, 137–154.
- Guidoboni, E., Comastri, A., 2005. Catalogue of Earthquakes and Tsunamis in the Mediterranean Area From the 11th to the 15th Century. SGA Storia Geofisica Ambiente srl, Bologna, p. 1037.
- Guidoboni, E., Comastri, A., Boschi, E., 2005. The “exceptional” earthquake of 3 January 1117 in the Verona area (northern Italy): a critical time review and detection of two lost earthquakes (lower Germany and Tuscany). *J. Geophys. Res.* 110 (B12), B12309. doi:10.1029/2005JB003683.
- Guidoboni, E., Ferrari, G., Tarabusi, G., Sgattoni, G., Comastri, A., Mariotti, D., Ciuccarelli, C., Bianchi, M.G., Valensise, G., 2019. CFT15Med, the new release of the catalogue of strong earthquakes in Italy and in the Mediterranean area. *Scientific Data* 6, 80. doi:10.1038/s41597-019-0091-9.
- Haddad, A., Antunes, V., Zahradnik, J., Lazar, M., Alcani, M., Gasperini, L., Polonia, A., Mazzini, A., Lupi, M., 2020. Tectonics of the Dead Sea fault driving the July 2018 seismic swarm in the Sea of Galilee (Lake Kinneret), Israel. *Journal of Geophysical Research: Solid Earth*. doi:10.1029/2019JB018963.
- Hovland, M., Judd, A.G., 1988. Seabed Pockmarks and Seepages. Publ. Graham and Trotman Inc., Sterling House, London (293 pp.).
- Kremer, K., Simpson, G., Girardclos, S., 2012. Giant Lake Geneva tsunamis in AD 563. *Nat. Geosci.* 5, 756–757. doi:10.1038/ngeo1618.
- Kremer, K., Gassner-Stamm, G., Grolimund, R., Wirth, S.B., Strasser, M., Fäh, D., 2020. A database of potential paleoseismic evidence in Switzerland. *J. Seismol.* 1–16.
- Lauterbach, S., Chapron, E., Brauer, A., Hüls, M., Gilli, A., Arnaud, F., Piccin, A., Nomade, J., Desmet, M., von Grafenstein, U., Participants, DeLakes, 2012. A sedimentary record of Holocene surface runoff events and earthquake activity from Lake Iseo (Southern Alps, Italy). *The Holocene* 22, 749–760.
- Lazar, M., Gasperini, L., Polonia, A., Lupi, M., Mazzini, A., 2019. Constraints on gas release from shallow lake sediments—a case study from the Sea of Galilee. *Geo-Mar. Lett.* 39 (5), 377–390.
- Lehmann, M.F., Bernasconi, S.M., Barbieri, A., McKenzie, J.A., 2002. Preservation of organic matter and alteration of its carbon and nitrogen isotope composition during simulated and in situ early sedimentary diagenesis. *Geochim. Cosmochim. Acta* 66 (20), 53–64.
- Livio, F., Berlusconi, A., Michetti, A.M., Sileo, G., Zerboni, A., Trombino, L., Cremaschi, M., Mueller, K., Vittori, E., Carcano, C.S., 2009. Active fault-related folding in the epicentral area of the December 25, 1222 (Io = IX MCS) Brescia earthquake (Northern Italy): seismotectonic implications. *Tectonophysics* 476, 320–335.
- Livio, F., Berlusconi, A., Zerboni, A., Trombino, L., Sileo, G., Michetti, A.M., Rodnight, H., Spötl, C., 2014. Progressive offset and surface deformation along a seismogenic blind thrust in the Po Plain foredeep (Southern Alps, Northern Italy). *Journal of Geophysical Research*. doi:10.1002/2014JB011112.
- Livio, F., Ferrario, M.F., Frigerio, C., Zerboni, A., Michetti, A.M., 2019. Variable fault tip propagation rates affected by near-surface lithology, and implications for fault displacement hazard assessment. *J. Struct. Geol.* doi:10.1016/j.jsg.2019.103914.
- Magri, G., Molin, D. (1986). I terremoti del 3 gennaio 1117 e 25 dicembre 1222. ENEA-RTI PAS-ISP-GEOLLO, (86) 2, Rapporto Tecnico ENEA, Roma (in Italian).
- Monegato, G., Scardia, G., Hajdas, I., Rizzini, F., Piccin, A., 2017. The Alpine LGM in the boreal ice-sheets game. *Sci. Rep.* 7, 1–8.
- Panizza, M., Slejko, D., Bartolomei, G., Carton, A., Castaldini, D., Demartini, M., Nicolich, R., Sauro, U., Semenza, E., Sorbini, L., 1981. Modello sismotettonico dell'area fra il Lago di Garda e il Monte Grappa. *Rend. Soc. Geol. It.* 4, 587–603 (in Italian).
- Piccoli, G., 1965. Rapporto tra gli allineamenti dei centri vulcanici paleogenici e le strutture tettoniche attuali nei Lessini. *Bollettino Società Geologica Italiana* 84, 141–157 (in Italian).
- Picotti, V., Prosser, G., Castellarin, A., 1995. Structures and kinematics of the Giudicarie-Val Trompia fold and thrust belt (central Southern Alps, Northern Italy). *Mem. Sci. Geol.* 47, 95–109.
- Polonia, A., Bonatti, E., Camerlenghi, A., Lucchi, R.G., Panieri, G., Gasperini, L., 2013. Mediterranean megaturbidite triggered by the AD 365 Crete earthquake and tsunamis. *Sci. Rep.* 3, 1285.
- Polonia, A., Nelson, C.H., Romano, Vaiani S.C., Colizza, E., Gasparotto, G., Gasperini, L., 2017. A depositional model for seismo-turbidites in confined basins based on Ionian Sea deposits. *Mar. Geol.* 384, 177–198.
- Preusser, F., Reiter, J.M., Schlüchter, C., 2010. Distribution, geometry, age and origin of overdeepened valleys and basins in the Alps and their foreland. *Swiss J. Geosci.* 103, 407–426.
- Ravazzi, C., Pini, R., Badino, F., De Amicis, M., Londeix, L., Reimer, P.J., 2014. The latest LGM culmination of the Garda Glacier (Italian Alps) and the onset of glacial termination. Age of glacial collapse and vegetation chronosequence. *Quat. Sci. Rev.* 105, 26–47.
- Rebesco, M., Stow, D., 2001. Seismic expression of contourites and related deposits: a preface. *Mar. Geophys. Res.* 22, 303–308.
- Rothwell, R.G., Thomson, J., Köhler, G., 1998. Low-sea-level emplacement of a very large Late Pleistocene ‘megaturbidite’ in the western Mediterranean Sea. *Nature* 392, 377–380.
- Rovida, A., Locati, M., Camassi, R., Lolli, B., Gasperini, P., 2020. The Italian earthquake catalogue CPTI15. *Bull. Earthq. Eng.* 18 (7), 2953–2984. <https://emidius.mi.ingv.it/CPTI15-DBMI15.v1.5/>.
- Salmaso, N., Decet, F., 1998. Interactions of physical, chemical and biological processes affecting the seasonality of mineral composition and nutrient cycling in the water column of a deep subalpine lake (Lake Garda, Northern Italy). *Archiv für Hydrobiologie* 142, 385–414.
- Saunier-Talbot, E., 2016. Paleolimnology as a tool to achieve environmental sustainability in the Anthropocene: an overview. *Geosciences* 6, 26. doi:10.3390/geosciences6020026.
- Sauro, U. (1974). Lineamenti geografici e geologici. In: Gerletti M. (Ed.), Indagini sul Lago di Garda. Quaderni I.R.S.A., 18, pp. 13–32 (in Italian).
- Sauro, U. (1992). Tra le montagne e nella pianura. In “Turri E. & Ruffo S. (a cura di) - Etsch - Adige, il fiume, gli uomini e la storia.” 29–59, CIERRE Ed. (in Italian). ISBN: (8885923402).
- Sauro, U., Zampieri, D., 2001. Evidence of recent surface faulting and surface rupture in the Fore-Alps of Veneto and Trentino (NE Italy). *Geomorphology* 40, 169–184.
- Schaefer, J., Denton, G., Barrell, D., Ivy-Ochs, S., Kubik, P., Andersen, B., Phillips, F., Lowell, T., Schlüchter, C., 2006. Near-synchronous interhemispheric termination of the last glacial maximum in mid-latitudes. *Science* 312, 1510–1513.
- Schmidt, G.A., Jungclaus, J.H., Ammann, C.M., Bard, E., Braconnot, P., Crowley, T.J., Delaygue, G., Joos, F., Krivova, N.A., Muscheler, R., Otto-Bliesner, B.L., Pongratz, J., Shindell, D.T., Solanki, S.K., Steinhilber, F., Vieira, L.E.A., 2012. Climate forcing reconstructions for use in PMIP simulations of the Last Millennium. *Geosci. Model Dev.* 5, 185–191.
- Semenza, E. (1974). La fase giudicariense, nel quadro di una nuova ipotesi sull'orogenesi alpina nell'area italo-dinarica. *Mem. S.G.I., XIII*, p.2, Pisa (in Italian).
- Serva, L., 1990. Il ruolo delle Scienze della terra nelle analisi di sicurezza di un sito per alcune tipologie di impianti industriali; il terremoto di riferimento per il sito di Viadana (MN). *Boll. Soc. Geol. Ital.* 109, 375–411 (in Italian).
- Shumway, G., 1960. Sound speed and adsorption studies of marine sediments by resonance method – part 1. *Geophysics* 25, 451–467.
- Strasser, M., Monecke, K., Schnellmann, M., Anselmetti, F.S., 2013. Lake sediments as natural seismographs: a compiled record of Late Quaternary earthquakes in Central Switzerland and its implication for Alpine deformation. *Sedimentology* 60, 319–341.
- Stucchi, M., Galadini, F., Rovida, A., Moroni, A., Albini, P., Mirto, C., Migliavacca, P., 2008. Investigation of pre-1700 earthquakes between the Adda and the Middle Adige river basins (Southern Alps). In: Fréchet, J., Meghraoui, M., Stucchi, M. (Eds.), *Historical Seismology*. Springer, Dordrecht, pp. 93–129. *Modern Approaches in Solid Earth Sciences*, vol. 2.
- Trombetta, G.L., Claps, M., Masetti, D., Ronchi, P., 2004. Geologia, stratigrafia e sedimentologia del Triassico Superiore dell'Alto Garda (Prealpi Bresciane fra il Lago di Garda e il Lago d'Idro). *Ann. Mus. civ. St. nat. Ferrara* 7, 3–50 (in Italian).

- Viganò, A., Scafidi, D., Ranalli, G., Martin, S., Della Vedova, B., Spallarossa, D., 2015. Earthquake relocations, crustal rheology, and active deformation in the central-eastern Alps (N Italy). *Tectonophysics* 661, 81–98.
- Wessel, P., Smith, W.H., 1998. New, improved version of Generic Mapping Tools released. *Eos, Transactions American Geophysical Union* 79, 579.

UNCORRECTED PROOF